

Morphology and Specific Surface Free Energies of Ruby Single Crystal Grown from Molybdenum Trioxide Flux Studied by Contact Angle of Liquid Droplets

Takaomi Suzuki,* Eiichi Iguchi, Katsuya Teshima, and Shuji Oishi

Department of Environmental Science and Technology, Faculty of Engineering,
Shinshu University, 4-17-1 Wakasato, Nagano 380-8553

Received July 26, 2006; E-mail: takaomi@gipwc.shinshu-u.ac.jp

Contact angles of water and formamide droplets on a ruby crystal grown from MoO_3 flux were determined. The specific surface free energies of the $(11\bar{2}3)$ and (0001) faces, calculated using the Fowkes approximation, were 48 ± 1 and $65 \pm 1 \text{ mN m}^{-1}$, respectively. The length of the normal lines from the center of the crystal to $(11\bar{2}3)$ and (0001) faces were 1.06 and 1.45 mm, respectively. The relationship between the specific surface free energy and the morphology of the crystal satisfies Wulff's relationship.

Specific surface free energy can be used to determine the stability of a crystal surface and the morphology of single crystal, and it can be described by Wulff's relationship,¹

$$\frac{\gamma_i}{h_i} = \text{constant}, \quad (1)$$

where γ_i is the specific surface free energy of the i -th (arbitrary) face of the crystal and h_i is the length of the normal line to the i -th face from Wulff's point in the crystal. In spite of theoretical significance, there are very few experimental approaches for measuring the specific surface free energy. So far, we have experimentally tried to determine the specific surface free energy of single crystals of chlorapatite, using the contact angles of liquids on the crystal surfaces.^{2–5} According to Eq. 1, the ratio of the specific surface free energy should be equal to that of the length of the perpendicular lines to the surface from Wulff's point, i.e., $h_i/h_j = \gamma_i/\gamma_j$. We have reported that the relationship between two different surfaces of chlorapatite, i.e., $(10\bar{1}1)$ and $(10\bar{1}0)$, roughly satisfied Wulff's relationship.⁵

Recently, we synthesized hexagonal bipyramidal ruby crystals from a MoO_3 flux.^{6,7} As well, lead compound fluxes, such as PbF_2 , $\text{PbO-B}_2\text{O}_3$, or PbO-PbF_2 produce ruby crystals with a platelike habit and well-defined (0001) faces.⁸ In this paper, we report the specific surface free energy of bipyramidal ruby crystals grown from a MoO_3 flux in order to explain the morphology of the bipyramidal ruby crystal.

Experimental

Ruby crystals were synthesized using a MoO_3 flux.^{6,7} The details of the synthesis of the sample crystal are described elsewhere.^{6,7} The form of ruby crystal was a hexagonal bipyramidal with $(11\bar{2}3)$ faces and small (0001) end faces. The sizes of the crystals were $\approx 3 \text{ mm}$ in length and $< 2 \text{ mm}$ in width. The synthesized crystal was sonicated with ethanol and thoroughly dried. A well-formed single crystal was fixed on a glass plate using a small piece of clay for contact angle measurement. The sample liquid was dropped onto the crystal using a micropipet. The droplets with

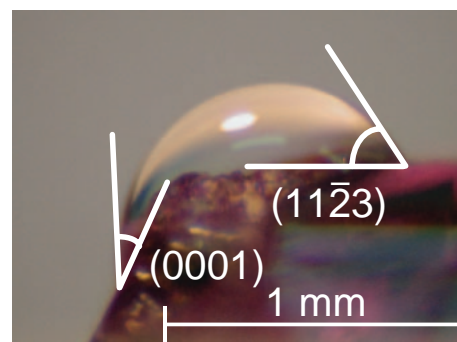


Fig. 1. A photograph of water droplet on the edge between the (0001) and $(11\bar{2}3)$ faces of ruby crystal.

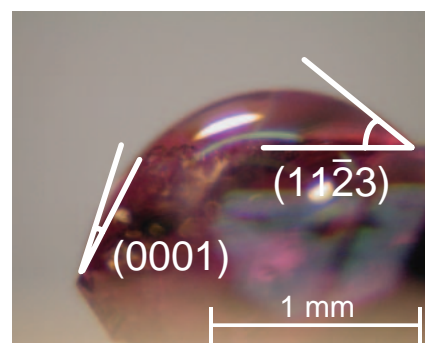


Fig. 2. A photograph of formamide droplet on the edge between the (0001) and $(11\bar{2}3)$ faces of ruby crystal.

a volume of $\approx 0.1 \text{ mm}^3$ were observed using a digital camera (Nikon COOLPIX 910) with a magnifying lens (Nikon $8 \times 20\text{D}$). Figures 1 and 2 show photographs of droplets of distilled water and formamide on the edge between the $(11\bar{2}3)$ and (0001) faces of a ruby crystal, respectively. Because the crystals were so small, it was difficult to settle a droplet onto a single face of the crystal. We attempted to place the droplet in the same position for each measurement. After each photograph with the droplet, the crystal

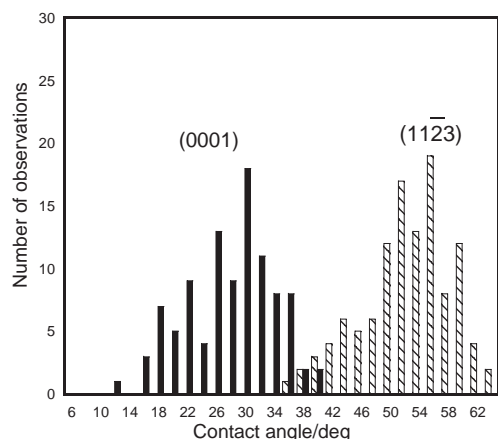


Fig. 3. Number of observations of contact angles, $\theta_{(0001)}$ and $\theta_{(11\bar{2}3)}$, for water droplets on ruby crystal.

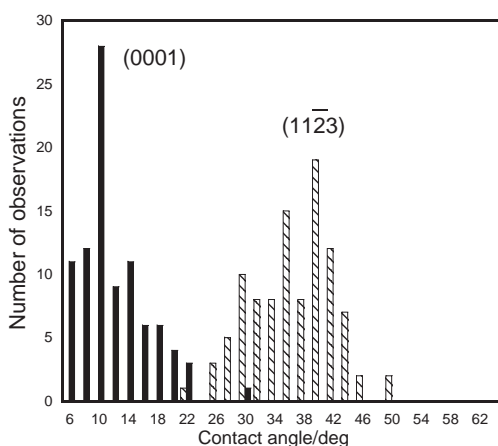


Fig. 4. Number of observations of contact angles, $\theta_{(0001)}$ and $\theta_{(11\bar{2}3)}$, for formamide droplets on ruby crystal.

was sonicated with ethanol again and well dried. We took more than 200 photographs and used the photos, in which the boundary between the liquid and solid was clearly recognized. The contact angles of the droplets on the $(11\bar{2}3)$ and (0001) faces, denoted as $\theta_{(11\bar{2}3)}$ and $\theta_{(0001)}$, respectively, were measured manually using a graduated ruler and printed photographs.

Results

The measured contact angles of water droplets on a ruby crystal are summarized in Fig. 3. The contact angle for the water droplet had a wide distribution on the $(11\bar{2}3)$ face, $\theta_{(11\bar{2}3)}$, with a peak at 56° , a minimum at 36° and a maximum at 64° . Likewise, the peak angle on the (0001) face, $\theta_{(0001)}$, was 30° , and the distribution range was $20^\circ \leq \theta_{(0001)} \leq 50^\circ$. The corresponding peaks of $\theta_{(11\bar{2}3)}$ and $\theta_{(0001)}$ for the formamide droplets, shown in Fig. 4, were 40° and 10° . The range of their distributions was $22^\circ \leq \theta_{(11\bar{2}3)} \leq 50^\circ$ and $6^\circ \leq \theta_{(0001)} \leq 30^\circ$. In summary, $\theta_{(11\bar{2}3)}$ was significantly larger than $\theta_{(0001)}$ for both liquids, and both contact angles for formamide were smaller than those for water.

Discussion

Though the error in the contact angle measurement was considered to be less than $\pm 1^\circ$, the distribution of the contact

angles was very wide, as shown in Figs. 3 and 4. Such a wide distribution of the contact angles was also observed in our previous study for chlorapatite crystals.^{3,5} If the surface of the crystal was ideally flat and uniform, the specific surface free energy should be uniquely determined and the distribution of the observed contact angles should converge to within the measurement error. However, the real surface has a lot of defects of atomic scale, such as steps, even though the electron microscope picture shows a smooth flat surface. The real specific surface free energy can be described as a combination of an ideal specific surface free energy of the terrace, γ_{terr} , and the step free energy, β , as

$$\gamma_s = \gamma_{\text{terr}} + L\beta \quad (2)$$

where L is density (length per unit area) of the step. γ_{terr} and β are characteristic for the face of the crystal, but L is not unique: probably the steps are randomly distributed on the surface. This random distribution of the step may cause the wide distribution in the observed contact angles of liquid droplets. In the real growing process of the crystal, the growth rate of each face is determined by its representative value of the specific surface free energies. Therefore, the most frequent value of the contact angles should reflect the effective specific surface free energy of the growing crystal surface.

The values of specific surface free energy, γ_s , can be obtained from the contact angle of the liquid, θ , using the Fowkes approximation,⁹ and Wu's harmonic and geometric mean equations¹⁰ as

$$\gamma_{LV}(1 + \cos \theta) = 4 \left(\frac{\gamma_{LV}^d \gamma_s^d}{\gamma_{LV}^d + \gamma_s^d} + \frac{\gamma_{LV}^p \gamma_s^p}{\gamma_{LV}^p + \gamma_s^p} \right), \quad (3)$$

$$\gamma_{LV}(1 + \cos \theta) = 2((\gamma_{LV}^d \gamma_s^d)^{1/2} + (\gamma_{LV}^p \gamma_s^p)^{1/2}), \quad (4)$$

where γ_{LV} is the surface tension of the liquid, γ_s^d and γ_s^p are the dispersion and polar components of the specific surface free energy of the solid, respectively, and γ_{LV}^d and γ_{LV}^p are those of the surface tension of the liquid, respectively. These equations are widely accepted for use in studies on the surface free energy of polymer surfaces.^{11–19} We have also used the equations for calculating of the specific surface free energies of chlorapatite crystals^{3,5} and have discussed the relationship between the specific surface free energy and the morphology of the crystals.³ The specific surface free energies of the $(11\bar{2}3)$ and (0001) faces were calculated using the most frequent value of contact angles measured for water and formamide. The polar and dispersed components of the liquid were taken from previously reported data.¹¹ The specific surface free energy for the (0001) face ($\gamma_{(0001)}$) was 66 mN m^{-1} from the harmonic mean equation and 64 mN m^{-1} from the geometric mean equation and that for the $(11\bar{2}3)$ face ($\gamma_{(11\bar{2}3)}$) was 49 mN m^{-1} from the harmonic mean equation and 47 mN m^{-1} from the geometric mean equation. The value of specific surface free energy calculated from the most frequent values of the contact angles for the $(11\bar{2}3)$ face was smaller than that for the (0001) face, which means that the former face is more stable than the latter face. The ratio of $\gamma_{(0001)}/\gamma_{(11\bar{2}3)}$ was 1.35. The $h_{(0001)}$ and $h_{(11\bar{2}3)}$, measured from the photograph, were 1.45 and 1.06 mm, respectively, as shown in Fig. 5. The ratio of length of the normal lines was $h_{(0001)}/h_{(11\bar{2}3)} = 1.37$. This agreement between the ratios of γ and h satisfy Wulff's relationship.

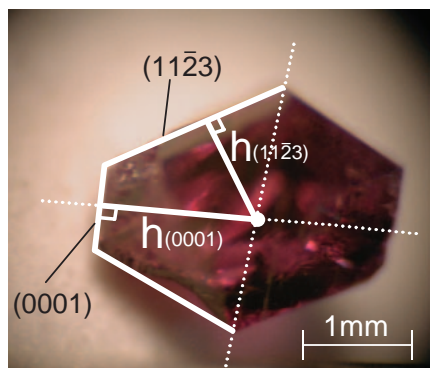


Fig. 5. Morphology of the observed ruby crystal.

Conclusion

The approximation of Fowkes and the geometric and harmonic means by Wu were used to calculate the specific surface free energy of a ruby single crystal from the contact angle of liquids on the surface. The experimentally obtained specific surface free energies satisfy Wulff's relationship, even with a grown shape crystal.

This research was supported by the CLUSTER of the Ministry of Education, Culture, Sports, Science and Technology.

References

- 1 M. v. Laue, *Z. Kristallogr.* **1944**, 105, 124.
- 2 T. Suzuki, G. Hirose, S. Oishi, *Mater. Res. Bull.* **2004**, 39, 103.
- 3 T. Suzuki, K. Nakayama, S. Oishi, *Bull. Chem. Soc. Jpn.* **2004**, 77, 109.
- 4 T. Suzuki, M. Shimuta, S. Oishi, *Bull. Chem. Soc. Jpn.* **2006**, 79, 427.
- 5 T. Suzuki, I. Kumeda, K. Teshima, S. Oishi, *Chem. Phys. Lett.* **2006**, 421, 343.
- 6 S. Oishi, K. Teshima, H. Kondo, *J. Am. Chem. Soc.* **2004**, 126, 4768.
- 7 K. Teshima, H. Kondo, S. Oishi, *Bull. Chem. Soc. Jpn.* **2005**, 78, 1259.
- 8 D. Elwell, H. J. Scheel, *Crystal Growth from High-Temperature Solutions*, Academic Press, London, **1975**.
- 9 F. M. Fowkes, *Ind. Eng. Chem.* **1964**, 56, 40.
- 10 S. Wu, *J. Polym. Sci., Part C* **1971**, 34, 19.
- 11 R. N. Shimizu, N. R. Demarquette, *J. Appl. Polym. Sci.* **2000**, 76, 1831.
- 12 D. Y. Kwok, C. N. C. Lam, A. Li, K. Zhu, R. Wu, A. W. Neumann, *Polym. Eng. Sci.* **1998**, 38, 1675.
- 13 J. Long, P. Chen, *Langmuir* **2001**, 17, 2965.
- 14 J. K. Spelt, D. Li, in *Applied Surface Thermodynamics*, ed. by A. W. Neumann, J. K. Spelt, Marcel Dekker, New York, **1996**, Chap. 5.
- 15 J. F. Oliver, C. Hoh, S. G. Mason, *Colloids Surf.* **1980**, 1, 79.
- 16 A. W. Neumann, *Adv. Colloid Interface Sci.* **1974**, 4, 105.
- 17 D. Li, A. W. Neumann, *J. Colloid Interface Sci.* **1992**, 148, 190.
- 18 D. Li, E. Moy, A. W. Neumann, *Langmuir* **1990**, 6, 885.
- 19 D. Y. Kwok, C. N. C. Lam, A. Li, A. W. Neumann, *J. Adhes.* **1998**, 68, 229.